HHS Public Access

Author manuscript

Prostate. Author manuscript; available in PMC 2019 November 04.

Published in final edited form as:

Prostate. 2017 July ; 77(10): 1066–1075. doi:10.1002/pros.23362.

The common parasite *Toxoplasma gondii* induces prostatic inflammation and microglandular hyperplasia in a mouse model

Darrelle L. Colinot[1], **Tamila Garbuz**[1,2], **Maarten C. Bosland**[3], **Liang Wang**[1], **Susan E. Rice**[4], **William J. Sullivan Jr**[1,2], **Gustavo Arrizabalaga**[1,2], **Travis J. Jerde**[1,4,5,iD]

[1]Department of Pharmacology and Toxicology, Indiana University School of Medicine, Indianapolis, Indiana

[2]Department of Microbiology and Immunology, Indiana University School of Medicine, Indianapolis, Indiana

[3]Department of Pathology, University of Illinois-Chicago, Chicago, Illinois

[4]Indiana University Melvin and Bren Simon Cancer Center, Indiana University School of Medicine, Indianapolis, Indiana

[5]Department of Urology/Indiana Basic Urological Research Program, Indiana University School of Medicine and Purdue University Center for Cancer Research, Indianapolis, Indiana

Abstract

Background—Inflammation is the most prevalent and widespread histological finding in the human prostate, and associates with the development and progression of benign prostatic hyperplasia and prostate cancer. Several factors have been hypothesized to cause inflammation, yet the role each may play in the etiology of prostatic inflammation remains unclear. This study examined the possibility that the common protozoan parasite *Toxoplasma gondii* induces prostatic inflammation and reactive hyperplasia in a mouse model.

Methods—Male mice were infected systemically with *T. gondii* parasites and prostatic inflammation was scored based on severity and focality of infiltrating leukocytes and epithelial hyperplasia. We characterized inflammatory cells with flow cytometry and the resulting epithelial proliferation with bromodeoxyuridine (BrdU) incorporation.

Results—We found that *T. gondii* infects the mouse prostate within the first 14 days of infection and can establish parasite cysts that persist for at least 60 days. *T. gondii* infection induces a substantial and chronic inflammatory reaction in the mouse prostate characterized by monocytic and lymphocytic inflammatory infiltrate. *T. gondii*-induced inflammation results in reactive hyperplasia, involving basal and luminal epithelial proliferation, and the exhibition of proliferative inflammatory microglandular hyperplasia in inflamed mouse prostates.

Correspondence. Travis J. Jerde, PhD, Associate Professor, Department of Pharmacology and Toxicology, Indiana University School of Medicine, A417 VanNuys Medical Sciences Building, 635 Barnhill Drive, Indianapolis, IN 46202. ttjerde@iupui.edu.
Travis J. Jerde http://orcid.org/0000-0002-1160-4665
Gustavo Arrizabalaga and Travis J. Jerde contributed equally to this study.

CONFLICTS OF INTEREST

None.

Conclusions—This study identifies the common parasite *T. gondii* as a new trigger of prostatic inflammation, which we used to develop a novel mouse model of prostatic inflammation. This is the first report that *T. gondii* chronically encysts and induces chronic inflammation within the prostate of any species. Furthermore, *T. gondii*-induced prostatic inflammation persists and progresses without genetic manipulation in mice, offering a powerful new mouse model for the study of chronic prostatic inflammation and microglandular hyperplasia.

Keywords

hyperplasia; inflammation; parasite; prostate; *Toxoplasma gondii*

1 INTRODUCTION

Prostate cancer and benign prostatic hyperplasia (BPH) are both very common and costly urological conditions in aging men. Prostatic carcinomas exist in up to 29% of men 30–40 years of age, and are found in 64% of men in their sixties.[1] The risk of death due to metastatic prostate cancer is now up to 1 in 30 in western countries.[2] Similarly, benign prostatic growth is a nearly ubiquitous process in aging men and is characterized by proliferation of epithelium and stroma in the periurethral and transition zones of the prostate. Nearly every man, regardless of race or ethnicity, will develop BPH and experience inconvenient, painful, and sometimes intolerable lower urinary tract symptoms, which range from hesitancy and weak stream to increased urgency and increased frequency, especially at night. No single causative factor has been identified for BPH or prostate cancer, though numerous factors have been proposed, including diet, endocrine signaling from androgens or estrogens, genetic susceptibilities, and exposure to environmental carcinogens. However, one pathological feature is dominant in proliferative prostatic diseases: continual and recalcitrant inflammation.[3]

Inflammation of the human prostate is a critical area of urological research due to its common concurrence with prostate cancer and BPH.[4–6] Prostatic inflammation is diagnosed histologically from the presence of inflammatory cells infiltrating the prostatic stroma, epithelium, and lumen of prostate glands.[7] In the transitional zone of the human prostate, the cellular nature inflammation is primarily lymphocytic with secondary accompanying macrophages juxtaposed to loci of reactive hyperplasia.[8] Additionally, inflammation in the prostate associates with dysplastic changes including focal disruption of the epithelium, polymorphisms of epithelial cell nuclei, and increased epithelial proliferation, and proliferative atrophy.[2,3]

Human prostatectomy specimens exhibit proliferating epithelial cells and activated inflammatory cells juxtaposed to neoplasia and hyperplastic glands. Numerous prostate disease susceptibility genes function in the inflammatory response.[4,5] Sustained cell proliferation in an environment rich in inflammatory cells, growth factors, and reactive stroma, potentiate prostatic epithelial growth.[9] Interleukins 1 and 6, tumor necrosis factor, and prostanoids all promote tumor cell growth in culture, and all are increased in both BPH and prostate cancer specimens relative to controls.[10–12] In addition, prostatic inflammation

is associated with more severe symptoms and an increased risk for clinical progression of BPH,[13] as there is a clear correlation of inflammation with BPH symptom severity.[14]

The origins of inflammation in the prostate are likely multi-factorial and may include bacterial colonization by culturable or non-culturable organisms,[15,16] viruses, environmental, and dietary components, systemic androgen and estrogens, associations with metabolic syndrome, and urinary reflux of any of these noxious stimuli into the prostatic ducts.[17] However, the role each may play in the etiology of human prostatic inflammation still remains unclear.

Toxoplasmosis and various pathologies correlated with chronic toxoplasmosis, such as systemic lupus erythematosus[18] and inflammatory bowel disease,[19] have an inflammatory component.[18–25] Toxoplasmosis is caused by the common parasite, *Toxoplasma gondii*, an obligate intracellular protozoan capable of infecting any nucleated mammalian or avian cell.[26] Serology testing has confirmed that almost 1/3 of the western population has been exposed to *T. gondii*, with certain populations showing an infection rate as high as 80%.[27,28] Humans can become infected through multiple routes, including the ingestion of oocysts deposited into the environment by felines (the definitive host) in their feces, ingestion of tissue cysts in the raw or undercooked meat of infected animals, and congenital transmission across the placenta. Upon initial infection, immune competent individuals may experience mild flu-like symptoms as the immune response prompts the rapidly replicating form of the parasite (tachyzoite) to convert into a latent tissue cyst form (bradyzoite). Bradyzoite tissue cysts, which can be found at high frequency in the brain and muscular tissue, allow *T. gondii* to persist as a lifelong chronic infection in the host.[29,30] Impervious to current drug treatments, the tissue cysts are not eradicated from the host and can reactivate into the proliferative form if immunity becomes compromised. Since the latent cyst stage of *T. gondii* had not been associated with symptomology or pathogenesis in the immunocompetent, little attention has been given to its presence in specific infected organs. In this report, we show for the first time that *T. gondii* promotes prostatic inflammation and the subsequent reactive hyperplasia in mice. Furthermore, we present a comprehensive characterization of a murine model of chronic prostatic inflammation, one which persists and progresses in severity without genetic manipulation.

2 MATERIALS AND METHODS

2.1 Parasites strains and culture

T. gondii parasites of strain PruΔhxprt + ldh2GFP (aka PruΔC32)[31] were grown on human foreskin fibroblasts (HFF) obtained from ATCC. HFFs were maintained in Dulbecco's medium supplemented with 10% heat-inactivated fetal bovine serum (FBS), 2 mM L-glutamine, 100 U/mL penicillin, and 100 μg/mL streptomycin in a humidified incubator at 37°C with 5% CO_2.

2.2 Animal infections

All mice used in this study were housed at the Indiana University School of Medicine under approval and supervision of the Animal Care and Use Committee of the Indiana University

School of Medicine in accordance with the National Institutes of Health Guide for the Care and Use of Laboratory Animals. Tachyzoites were isolated from host cells immediately prior to infection by scraping host cell monolayers, passing through a 27.5 gauge syringe three times, and filtering through a 3 μm pore filter. A 6–8-week-old male CBA/J mice were intraperitoneally injected with either sterile PBS as vehicle control or 40 000 PruΔC32 tachyzoites. Control or experimental groups were randomized to sacrifice and process at either 14, 28, or 60 days post infection. Mice were intraperitoneally injected 2 h prior to sacrifice with 250 μL of 3.1 mg/mL bromodeoxyuridine. Infection was verified by testing mouse sera in immunoblotting assays.

2.3 Tissue harvesting and processing

Freshly harvested prostates were dissected into individual ventral, dorsal lateral, and anterior lobes then bilaterally cut in two. One lobe of each region was fixed in 10% neutral buffered formalin for at least 24 h. The other portions were flash frozen in liquid nitrogen then stored in −80°C for protein extraction. Fixed tissues were processed via dehydration through graded ethanol and xylene, then embedded into paraffin blocks. Five micrometre sections were cut by microtome then heat fixed to glass slides.

2.4 Immunofluorescence

Heat fixed paraffin embedded sections were prepared for immunohistochemical analysis as previously described.[32] Slides were incubated overnight at 4°C with one or a combination of the following, diluted in blocking buffer (10% normal donkey serum, 1% bovine serum albumin in PBS-T): mouse anti-GFP (CAT#: am10009a, Abgent) at 1:50, rabbit anti-pan-cytokeratin at 1:50 (Novus, NBP2-29429), rhodamine-labeled *Dolichos biflorus agglutinin* at 1:350 (CAT #: RL-1032, Vector Labs), rabbit anti-BAG1 at 1:100 (provided by Dr Laura Knoll),[33] mouse anti-CD45 (CAT#: 136-4B5, Cell Signaling) at 1:100, mouse anti-CD3ε (CAT#: MA1-7630, Thermo) at 1:100, rat anti-F4-80 (CAT#: MA1-91124, Thermo), mouse anti-CD20 (CAT#: MA1-7634, Thermo), mouse anti-Bromodeoxyuridine at 1:200 (CAT#: 5292, Cell Signaling), rabbit anti-Keratin 5 at 1:1000 (CAT#: PRB-160P, Covance), or mouse anti-cytokeratin 8 (CAT#: NB120-9287, Novus). After sections had been washed with PBS-T, Invitrogen Alexa Fluor 488 or 594 anti-mouse, rabbit, or rat IgG secondary antibodies at 1:200 were applied for 1 h at room temperature in the dark. After serial washes with PBS-T, sections were incubated with 20 μg/mL Hoechst 33342 in PBS-T for 10 min to visualize nuclei. Coverslips were mounted using PermaFluor Mountant media (CAT#: TA-030-FM, Thermo). Slides were viewed using a Nikon Eclipse E100080i microscope and digital images were captured with Hamamatsu C4742-95 charge-coupled device camera using NIS elements software.

2.5 Inflammatory scoring

Tissue sections were stained with hematoxylin and eosin and viewed on a Leica DM 2500 microscope. Three random 10× images/mouse were taken using a Leica 2500 microscope and DCF425C Camera and analyzed with LASX software. Inflammatory response of the DLP, AP, and VP were scored in a blinded manner and graded based on severity and focality of inflammatory infiltrate and epithelial hyperplasia as previously described.[34]

2.6 Protein extraction

Flash frozen prostate tissues were placed into 1.5 mL screw cap tubes with 500 μL ice-cold lysis buffer (0.12 g Tris base, 0.9g NaCl in 100 mL of ddH_20, pH to 8.0, Halt Protease/Phosphatase Inhibitor Cocktail: 1:100) (CAT#: 78446, Thermo) and minced into ~1 mm pieces. Prostates were homogenized using a Power Gen 125 on ice for no longer than 5 min. A total of 1% v/v of Triton-X was added to each vial and slurries were incubated on ice for one hour with periodic vortexing. Vials were then centrifuged at 14 500 rpm for 10 min. The supernatant was removed and stored in −80°C until use.

2.7 Western blotting

Protein concentrations were quantified by bicinchoninic acid colorimetric assay. Absorbances were determined using a BioTek Synergy HI hybrid reader and Gen5 2.0 software. Equal amounts of proteins were resolved by SDS-PAGE and transferred to nitrocellulose membranes. To prevent nonspecific binding, membranes were incubated in blocking buffer (5% milk, 5% BSA, in PBS-T) overnight at 4°C. Membranes were incubated with mouse anti-GFP at 1:2000 (CAT#: AM1009A, Abgent) and mouse anti-β-actin at 1:2000 as a loading control (CAT#: 3700, Cell signaling), diluted in 5% BSA and PBS-T overnight at 4°C. Membranes were washed and then incubated with anti-mouse IgG horseradish peroxidase linked secondary antibody at 1:5000 (CAT#: 7076S, Cell Signaling) in 5% Milk 2% BSA in PBS-T. For visualization, membranes were treated with Super Signal West Femto and Pico Chemiluminescent Substrate (CAT# 34095, 34078, Thermo) developing reagents at 1:10 and allowed to incubate for 5 min. Developed GFP blots were exposed to films for 5 min and Actin blots were exposed for 1 min before processing.

2.8 Flow cytometry

Mouse prostates were processed into single-cell suspensions and intracellular and extracellular markers of interest were labeled as previously described.[35] Before applying primary antibodies to the cells, non-specific Fc Receptor binding was blocked using 0.5 μg/million cells of purified functional grade anti-mouse CD16/CD32 (CAT#: 16-0161, eBioscience) diluted in 100 μL of PBS, and incubated on ice for 30 min. After surface staining, cells were fixed using Cytofix/Cytoperm Fixation and Permeabilization Solution (CAT#: 554722, BD Bioscience) either overnight at 4°C (surface staining experiments) or (intracellular staining) at room temperature for 30 min. After staining, cells were resuspended in Cytofix/Cytoperm Fixation and Permeabilization Solution and transferred into a sterile 5 mL Polystyrene round-bottom tube with cell strainer cap (CAT#: 352235, Falcon) and stored overnight at 4°C. Analysis was carried out at the Indiana University Simon Cancer Center Flow Cytometry Research Core Facility on a BD Biosciences FACSAria. Analysis was performed using FloJo Software.

Single-color compensation controls for each experiment were prepared using UltraComp eBeads (CAT#: 00-4222, eBioscience). Autofluorescence was controlled for using unstained cells and fluorochrome conjugated isotype antibodies.

T-cell and dendritic cell analysis was performed using antibodies at the following concentrations: 0.5 μg/million cells rat IgG2b K, mouse anti-CD45 eFluor 450 (CAT#:

48-0451, eBioscience); 0.125 μg/million cells rat IgG2b K, mouse anti-CD3ε PE (CAT#: 12-0031, eBioscience); 0.125 μg/million cells rat IgG2a K, mouse anti-CD8α PE-Cyanine5.5 (CAT#: 35-0081, eBioscience); 0.125 μg/million cells rat IgG2b K, mouse anti-CD11c Alexa Fluor 488 (CAT#: 53-0144, eBioscience). The following isotype controls were used at the same concentration as its corresponding fluorophore conjugated primary antibodies: rat IgG2b K isotype control eFluor 450 (CAT#: 48-4031, eBioscience), Armenian hamster IgG isotype control PE (CAT#: 12-4888, eBioscience), rat IgG2a K isotype control PE-Cyanine5.5 (CAT#: 35–4321, eBioscience), and Armenian hamster IgG isotype control Alexa Fluor 488 (CAT#: 53-4888, eBioscience). Monocyte, macrophage, and B-cell analysis, was performed using antibodies at the following concentrations: 0.5 μg/million cells rat IgG2b K, mouse anti-CD45 eFluor 450 (CAT#: 48-0451, eBioscience); 0.25 μg/million cells rat IgG2a mouse anti-CD20PE (CAT#:12-0201, eBioscience), 0.5 μg/million cells rat IgG2a K, mouse anti-F4/80 antigen APC-eFluor 780 (CAT#: 47-4801, eBioscience), 10 μL/million cells polyclonal Sheep IgG anti-human/mouse Arginase 1 Fluorescein-conjugated (CAT#: IC5868F, R&D Systems); 0.06 μg/million cells Rat IgG2a K mouse anti-NOS2 PE-eFluor 610 (CAT#: 61-5920, eBioscience). The following isotype controls were used at the same concentration as its corresponding fluorophore conjugated primary antibody: rat IgG2b K Isotype Control eFluor 450 (CAT#: 48-4031, eBioscience), rat IgG2a K isotype control PE (CAT#: 12-4321, eBioscience), rat IgG2a K isotype control APC-eFluor 780, normal sheep IgG Fluorescein isotype control (CAT#: IC016F, R&D Systems), and rat IgG2a K isotype control PE-eFluor 610 (CAT#: 61-4321-82, eBioscience).

3 RESULTS

3.1 *T. gondii* localizes to the mouse prostate and establishes a chronic infection

To determine if *T. gondii* establishes a chronic infection (ie, forms bradyzoite tissue cysts) in the mouse prostate, male CBA/J mice were injected intraperitoneally with either 40 000 parasites or sterile PBS for the uninfected controls. This parasite background has been engineered to express GFP during the bradyzoite stage (PruΔhxprt + ldh2GFP) to facilitate identification of tissue cysts.[31] Prostates were assessed for the presence of various parasite-specific markers at 14 days post infection (DPI), at which time the infection is mostly in the acute tachyzoite stage, and at 28 and 60 DPI to monitor chronic infection.[29,30] Using Western blot GFP was detected in infected mice at all three time points of harvest, but was absent in the uninfected controls (Fig. 1A). We next analyzed prostate tissues by immunofluorescence assay (IFA) and costained prostates with rhodamine conjugated-*Dolichos biflorus agglutinin* (DBA), a lectin that binds terminal α-N-acetylgalactosamine residues on the parasite's tissue cyst wall and GFP.[36] Structures exhibiting the characteristic staining pattern for tissue cysts were found at each time point (Fig. 1B). To further confirm that the GFP/DBA-positive structures in the prostates of infected mice were parasite tissue cysts, we co-stained prostate samples with DBA and bradyzoite antigen 1 (BAG1), a bradyzoite-specific heat shock protein (Fig. 1C).[33] Structures staining with both reagents were observed (Fig. 1C), indicating the presence of bradyzoite cysts in the infected prostate samples. We did not see DBA staining in uninfected mice, or in prostates of *Escherichia coli* 1677 instilled C57/B6 mice, indicating that the presence of DBA staining is specific to *T. gondii* and not a general effect of infection. Collectively, these results indicate that *T. gondii*

chronically encysts in the mouse prostate and can persist in this organ for at least 60 days post infection.

3.2 *T. gondii* infection induces chronic prostatic inflammation

We next sought to determine if *T. gondii* infection caused inflammation in the mouse prostate. We assessed the presence of inflammatory infiltrates in longitudinal sections from infected or control prostates at 14, 28, and 60 DPI using hematoxylin and eosin (H&E) stain. Infiltrating leukocytes were detected in all samples from infected animals and appeared to be significantly increased in numbers compared to uninfected animals (Fig. 2A). To quantitate this effect, we used an established scoring system[34] that measures inflammatory infiltrate based on the intensity, severity and focality. *T. gondii* induced a significant inflammatory reaction in all prostatic lobes at 14 and 28 DPI relative to uninfected age-matched vehicle control mice (Fig. 2B). All lobes exhibited similar inflammatory distribution and intensity throughout the time course of infection. At 14 DPI each lobe exhibited moderate inflammatory infiltrate, however; the dorsal lateral prostate (DLP) lobes exhibited the most pronounced time-dependent increase in inflammatory score, progressing from a score of 5.04 at 14 DPI to a score of 7.17 by 60DPI (Fig. 2B). These data indicate that *T. gondii* infection in the prostate induces chronic inflammation in all lobes of the prostate, which increases in severity during persistent infection.

3.3 *T. gondii* induces a predominantly T-cell immune response in the prostate

As the DLP was found to have the most reproducible and consistent presence of leukocytes by H&E staining, we chose this lobe for further characterization of the inflammatory response to *T. gondii* infection of the prostate. We probed for lymphocytic and monocytic markers CD20, F4-80, and CD3 by immunofluorescence to identify B lymphocytes, monocytes, and lymphocytes, respectively (Fig. 3A). To quantify individual immune cell types, we analyzed whole prostates by flow cytometry. As predicted by our immunofluorescence assays, there was a significant increase the percent of immune cells as a proportion of total live cells (identified by the pan-leukocyte marker, CD45) in infected animals relative to vehicle treated control (16.43% infected vs 8% control; $P = 0.0026$) (Fig. 3B). This increase is primarily attributed to a significant increase of T-lymphocytes as identified by their expression of CD3 (8.2% infected vs 2% control; $P = 0.0106$) and dendritic cells identified as CD11c and CD8α positive (0.48% con vs 1.28% infected vs 0.48% control; $P = 0.0006$) (Fig. 3B).

In total, the $CD45^+$ cell population of infected prostates consisted of 49% T-lymphocytes, 27% monocytes, 16% B cells, and 8% dendritic cells. The $CD45^+/F4\text{-}80^+$ monocyte population consisted primarily of non-polarized monocytes, as 95% failed to express the M1 marker NOS2 or the M2 marker Arg1. However, of the polarized monocytes, NOS2-expressing M1 macrophages outnumbered Arg1-expressing M2 macrophages by a 4 to 1 ratio in infected mice. Collectively, these experiments show that chronic *T. gondii* infection in the prostate elicits a substantial T-cell dominated inflammatory reaction.

3.4 *T. gondii* induces reactive epithelial hyperplasia

As inflammatory infiltrate contributes to the release of numerous pro-inflammatory cytokines and chemokines that promote the establishment of a reactive microenvironment that results in reactive epithelial hyperplasia, we sought to determine if *T. gondii* infection of the prostate results in reactive hyperplasia. Infected and uninfected age-matched control prostates were evaluated for epithelial hyperplasia, which is defined as the multi-layering of epithelial cell layers and dysplasia of expanded basal or cuboidal cells juxtaposed to inflammatory infiltrate (Fig. 4A).[37] Significant levels of hyperplasia were detected in all sections from infected animals, an observation that was quantified using the scoring system described by Boehm et al.[34] During acute (14 DPI) and early chronic (28 DPI) *T. gondii* infection, the VP (4.98, 3.94, respectively) and AP (4.62, 3.66, respectively) exhibited a substantial hyperplastic response. At 60 DPI, hyperplasia reached a score of 5.78 in the VP and 6.73 in the AP. In the DLP, hyperplasia severity increased from 4.27 during acute infection, to 6.83 by 60 DPI (Fig. 4B). These findings suggest that *T. gondii* establishes a chronic inflammatory microenvironment, leading to reactive epithelial hyperplasia in all lobes of the mouse prostate.

As the DLP exhibited the most reproducible, progressive, and pronounced hyperplastic response within the prostate, this lobe was selected for further characterization. To quantify epithelial proliferation, control and infected mice were injected with bromodeoxyuridine (BrdU) to label replicating cells, and the prostates were harvested 2 h later. We visualized BrdU incorporation into replicating DNA by immunofluorescence and found that *T. gondii* infection significantly increased the ratio of proliferating epithelial cells at all time points relative to uninfected controls (Fig. 5A,B). These results parallel the histological epithelial hyperplasia scores, and further demonstrate that *T. gondii*-induced inflammation elicits reactive hyperplasia. Proliferating cells of the epithelial compartment were confirmed as epithelial by pan-cytokeratin staining (Fig. 5A) that clearly demonstrated BrdU+/PanCK+ cell populations. The possibility of BrdU+ infiltrating leukocytes was eliminated by co-staining BrdU with CD45; this experiment failed to show any dual positive cells, (data not shown) eliminating inflammatory infiltrate as the potential source of BrdU+ cells.

To determine the lineage of the epithelial cells present in the hyperplastic regions, we probed sections from infected and uninfected prostates for markers of basal cells (cytokeratin 5, CK5) and luminal cells (cytokeratin 8, CK8).[38] Numerous foci of both luminal and basal hyperplasia were observed in the hyperplastic regions of infected mice (Fig. 5C). Proposed transit amplifying cells (TAC), which express both basal and luminal epithelial cytokeratins (CK5 and CK8),[39] were prominent in infected prostates but were rarely observed in uninfected control mice. These data indicate that TAC populations increase in response to infection.

Careful inspection of H&E stained sections revealed a unique histological patterning only observed in infected prostates. At 28 DPI we began to observe the formation of small, round, and connected glandular structures within the epithelial compartment of inflamed prostates (Fig. 6). These small micro-glandular formations remained contained within the basement membrane and may maintain their functionality as evidenced by proteinaceous fluid (Fig. 6) in their lumens. Additionally, substantial inflammatory infiltrate was commonly juxtaposed

to these regions of microglandular hyperplasia. This phenotype was absent in aged-matched uninfected mice, and is observed in 13 out of 16 infected prostates at 28 days and is fully penetrant at 60 DPI (6/6). These observations indicate that chronic *T. gondii* infection elicits proliferative inflammatory microglandular hyperplasia in the mouse prostate.

4 DISCUSSION

In this study, we show that *T. gondii* forms bradyzoite tissue cysts in the mouse prostate that are associated with the induction of chronic inflammation resulting in reactive hyperplasia. The model developed using *T. gondii*-infected mice should prove useful for the study of inflammation-induced hyperplasia of the prostate. In order to characterize the time-course and severity of *T. gondii*-induced prostatic inflammation, we employed the blinded scoring system previously reported by Boehm et al.[34] In this analysis, we show that *T. gondii*-induced inflammation is progressive in severity over time, which was found to be most pronounced in the DLP. Our data indicate that the prostatic inflammatory infiltrate are primarily T-cells and dendritic cells. These results are in agreement with previous reports of the immune response to *T. gondii* in other organs, such as the brain.[40] *Toxoplasma* is known to trigger the expression of dendritic cell-recruiting chemokines, essential in ensuring host survival.[41] During acute infection, dendritic cells produce IL-12, used in cross-talk with T-cells signaling them to produce INFγ. T-cells are necessary for controlling parasite burden and enabling host survival during toxoplasmosis.[40] T-cells are also implicated in the pathology of BPH and are commonly found juxtaposed to hyperplastic regions.[37] Future studies will be directed at fully characterizing the cytokine component of *T. gondii*-induced inflammation and hyperplasia in the prostate.

T. gondii infection results in the establishment of a chronic reactive inflammatory microenvironment in the prostate. During normal repair and recovery homeostatic processes, cells will eliminate damage due to noxious stimuli, stimulate epithelial regeneration, and stromal remodeling, promote angiogenesis to complete healing, and restore normal tissue function. Following these events, inflammation normally subsides.[42] However, in cases in which the immune system becomes deregulated, or the noxious stimuli or infection persists, the inflammation can become chronic by a self-sustaining vicious cycle. *T. gondii* infection induced a reactive microenvironment with substantial proliferation and hyperplasia of both luminal and basal epithelial compartments, involving the expansion of transit amplifying cells, the proliferative cells implicated in repair and recovery. Inflammation in this model resulted in hyperplasia and expansion of the glandular epithelium in a microglandular architecture. These microglandular hyperplastic regions exhibit an especially high density of BrdU-labeled proliferating cells, and exist in microenvironments that exhibit inflammation. This phenotype has never been observed in non-genetically modified or hormone manipulated rodents. The only reported example of this atypical hyperplasia has been observed for rats treated with exogenous estradiol and testosterone,[43,44] suggesting a hormonal angle to the mechanism of *T. gondii*-driven hyperplasia. Finally, it is notable that both inflammation and hyperplasia persist and progress at least as long as 60 days in this model. It is not clear why inflammation and hyperplasia may worsen at such chronic time points, but *T. gondii* infection typically exhibits recurrent reactivation from its cyst (bradyzoite) into its lytic (tachyzoite) life stages. It is possible that this later reactivation of

the tachyzoite stage at later time points promotes a continuing of the inflammatory response in the prostate. Future studies will be directed at answering this complex question, as well as determining how long *T. gondii* infection persists in the prostate. Infections of greater than 1 year could be resolved, or could be associated with more severe prostate disease, and or future work will answer this critical question.

Based on our results, we propose that *T. gondii*-infected mice can serve as a powerful new model of prostatic inflammation, one that is chronic and does not require the use of genetically modified mouse strains. The inflammation induced in this model is similar to human inflammation in that the dominant feature is the presence of T-cells and secondary macrophages and it slowly builds over time. Several mouse models of prostatic inflammation have been developed that have greatly increased our understanding of its implication in prostatic disease. Unfortunately, each of the existing models have limitations and do not fully recapitulate the human condition. The bacterial strains often used in animal models are relatively rarely associated with prostatic infection in the male human population.[34,45–48] Additionally, some bacterial models require microbial strains which are not readily available and/or require laborious culturing conditions. Bacterial models also rely on a difficult and potentially damaging instillation techniques of transurethral instillation. Importantly, chronic inflammation induced by bacterial models in non-genetically modified mice are not fully penetrant, do not affect all lobes, and have not yet been fully characterized and quantified. Genetically engineered mice such as the POET-3 autoimmune mouse model require particular background strains and back-breeding of protein knockouts onto the genetic strain of inflammation, which is costly and time consuming.[35,49] Additionally, hormone models yield many off-target and systemic effects making data interpretation difficult. Finally, each of the models produce variable responses.[34,35,46–50]

It has become increasingly accepted that inflammation is a causative and driving factor of prostate diseases such as BPH and prostate cancer.[2,3,6,50] However, the source of inflammation has not yet been fully elucidated and the origin of chronic prostatic inflammation has proved elusive. There was no precedence in the literature suggesting that *T. gondii* induces prostatic inflammation, however; since *T. gondii* is a ubiquitous pathogen that can persist in a variety of tissues and is associated with chronic inflammation, we hypothesized that it could be an inducer of prostatic inflammation relevant to the development of human urogenital diseases. Our data support future prospective studies involving analysis of *T. gondii* encystation in the human prostate and serological testing of symptomatic BPH patients and those with pathologically confirmed prostate cancer are warranted.

Acknowledgments

We gratefully acknowledge Dr Susan Perkins for performing all statistical analysis in this manuscript. We also acknowledge Dr Laura Knoll for providing the Bag1 antibody. Finally, sincerest thanks are extended to the members of the Biology of Intracellular Pathogens group at IUSM as well as current and past Jerde lab members for their assistance and feedback in this project: David McIlwain, Jordi Van Iersel, and Yamarie Jallow. This work was funded by National Institutes of Health-NIDDK (DK092366-01A1); Dr Susan Perkins—statistical support, is funded by National Institutes of Health-NCI (P30 CA082709-16).

References

1. Sakr WA, Grignon DJ, Crissman JD, et al. High grade prostatic intraepithelial neoplasia (HGPIN) and prostatic adenocarcinoma between the ages of 20–69: an autopsy study of 249 cases. In Vivo. 1999; 8:439–443.
2. Jemal A, Thomas A, Murray T, Thun M. Cancer statistics, 2002. CA Cancer J Clin. 2002; 52:23–47. [PubMed: 11814064]
3. Nelson WG, De Marzo AM, Isaacs WB. Prostate cancer. N Engl J Med. 2003; 349:366–381. [PubMed: 12878745]
4. Rokman A, Ikonen T, Seppala EH, et al. Germline alterations of the RNASEL gene, a candidate HPC1 gene at 1q25, in patients and families with prostate cancer. Am J Hum Genet. 2002; 70:1299–1304. [PubMed: 11941539]
5. Xu J, Zheng SL, Komiya A, et al. Germline mutations and sequence variants of the macrophage scavenger receptor 1 gene are associated with prostate cancer risk. Nat Genet. 2002; 32:321–325. [PubMed: 12244320]
6. Delongchamps NB, DelaRoza G, Chandan V, et al. Evaluation of prostatitis in autopsied prostates—is chronic inflammation more associated with benign prostatic hyperplasia or cancer? J Urol. 2008; 179:1736–1740. [PubMed: 18343414]
7. Cotran, RS, Kumar, V, Robbins, SL. Prostatitis. In: Robbins, SL, editor. Robbins' Pathologic Basis of Disease. 6. Philadelphia: WB Saunders; 1999. 1025–1027.
8. De Marzo AM, Meeker AK, Zha S, et al. Human prostate cancer precursors and pathobiology. Urology. 2003; 62:55–62.
9. De Marzo AM, Marchi VL, Epstein JI, Nelson WG. Proliferative inflammatory atrophy of the prostate: implications for prostatic carcinogenesis. Am J Pathol. 1999; 155:1985–1992. [PubMed: 10595928]
10. Ricote M, García-Tuñón I, Bethencourt FR, Fraile B, Paniagua R, Royuela M. Interleukin-1 (IL-1alpha and IL-1beta) and its receptors (IL-1RI, IL-1RII, and IL-1Ra) in prostate carcinoma. Cancer. 2004; 100:1388–1396. [PubMed: 15042672]
11. Culig Z, Puhr M. Interleukin-6: a multifunctional targetable cytokine in human prostate cancer. Mol Cell Endocrinol. 2012; 360:52–58. [PubMed: 21664423]
12. Sciarra A, Mariotti G, Salciccia S, et al. Prostate growth and inflammation. Steroid Biochem Mol Biol. 2008; 108:254–260.
13. Nickel JC, Roehrborn CG, O'leary MP, Bostwick DG, Somerville MC, Rittmaster RS. Examination of the relationship between symptoms of prostatitis and histological inflammation: baseline data from the REDUCE chemoprevention trial. J Urol. 2007; 178:896–900. [PubMed: 17632164]
14. Nickel JC, Roehrborn CG, O'Leary MP, Bostwick DG, Somerville MC, Rittmaster RS. The relationship between prostate inflammation and lower urinary tract symptoms: examination of baseline data from the REDUCE trial. Eur Urol. 2008; 54:1379–1384. [PubMed: 18036719]
15. Krieger JN, Riley DE. Prostatitis: what is the role of infection. Int J Antimicrob Agents. 2002; 19:475–479. [PubMed: 12135836]
16. Hochreiter WW, Duncan JL, Schaeffer AJ. Evaluation of the bacterial flora of the prostate using a 16S rRNA gene based polymerase chain reaction. J Urol. 2000; 163:127–130. [PubMed: 10604329]
17. De Marzo AM, Platz EA, Sutcliffe S, et al. Inflammation in prostate carcinogenesis 2007. Nat Rev Cancer. 7:256–269. [PubMed: 17384581]
18. Berkun Y, Zandman-Goddard G, Barzilai O, et al. Infectious antibodies in systemic lupus erythematsus patients. Lupus. 2009; 8:1129–1135.
19. Lidar M, Langevitz P, Barzilai O, et al. Infectious serologies and autoantibodies in inflammatory bowel disease. Ann N Y Acad Sci. 2009; 1173:640–648. [PubMed: 19758210]
20. Fratamico, PM, Smith, JL, Brogden, KA. Sequelae and Long-Term Consequences of Infection Diseases. Washington DC: ASM Press; 2009.

21. Carter CJ. Toxoplasmosis and polygenic disease susceptibility genes: extensive *Toxoplasma gondii* host/pathogen interactome enrichment in nine psychiatric or neurological disorders. J Pathogens. 2013; 2012:965046.
22. Lidar M, Lipschitz N, Langevitz P, et al. Infectious serologies and autoantibodies in Wegener's granulomatosis and other vasculitides: novel associations disclosed using the Rad BioPlex 2200. Ann N Y Acad Sci. 2009; 1173:649–657. [PubMed: 19758211]
23. Portugal LR, Fernandes LR, Alvarez-Leite JI. Host cholesterol and inflammation as common key regulators of toxoplasmosis and artherosclerosis development. Expert Rev Anti Infect Ther. 2009; 7:807–819. [PubMed: 19735223]
24. Shapira Y, Agmon-Levin N, Selmi C, et al. Prevalence of anti-toxoplasma antibodies in patients with autoimmune diseases. J Autoimmun. 2012; 39:112–116. [PubMed: 22297145]
25. Flegr J, Prandota J, Sovic kova M, Israili ZH. Toxoplasmosis—a global threat. Correlation of latent toxoplasmosis with specific disease burden in a set of 88 countries. PLoS ONE. 2014; 9:e90203. [PubMed: 24662942]
26. Dubey JP. The history of *Toxoplasma gondii*—the first 100 years. J Eukaryot Microbiol. 2008; 55:467–475. [PubMed: 19120791]
27. Tenter AM, Heckeroth AR, Weiss LM. *Toxoplasma gondii*: from animals to humans. Int J Parasitol. 2000; 30:1217–1258. [PubMed: 11113252]
28. Pappas G, Roussos N, Falagas ME. Toxoplasmosis snapshots: global status of *Toxoplasma gondii* seroprevalence and implications for pregnancy and congenital toxoplasmosis. Int J Parasitol. 2009; 39:1385–1394. [PubMed: 19433092]
29. Zenner L, Foulet A, Caudrelier Y, et al. Infection with *Toxoplasma gondii* RH and prugniaud strains in mice, rats and nude rats: kinetics of infection in blood and tissues related to pathology in acute and chronic infection. Pathol Res Pract. 1999; 195:475–485. [PubMed: 10448664]
30. Di Cristina M, Marocco D, Galizi R, Proietti C, Spaccapelo R, Crisanti A. Temporal and spatial distribution of *Toxoplasma gondii* differentiation into bradyzoites and tissue cyst formation *in vivo*. Infect Immun. 2008; 76:3491–3501. [PubMed: 18505811]
31. Singh U, Brewer JL, Boothroyd JC. Genetic analysis of tachyzoite to bradyzoite differentiation mutants in *Toxoplasma gondii* reveals a hierarchy of gene induction. Mol Microbiol. 2002; 44:721–733. [PubMed: 11994153]
32. Jerde TJ, Mellon WS, Fischer SM, Liebert M, Bjorling DE, Nakada SY. Suppression of 15-hydroxyprostaglandin dehydrogenase messenger RNA concentration, protein expression, and enzymatic activity during human ureteral obstruction. JPET. 2004; 309:398–403.
33. Bohne W, Gross U, Ferguson DJP, Heesemann J. Cloning and characterization of a bradyzoite-specifically expressed gene (hsp30/ bag1) of *Toxoplasma gondii*, related to genes encoding small heat-shock proteins of plants. Mol Microbiol. 1995; 16:1221–1230. [PubMed: 8577255]
34. Boehm BJ, Colopy SA, Jerde TJ, Loftus CJ, Bushman W. Acute bacterial inflammation of the mouse prostate. Prostate. 2012; 72:307–317. [PubMed: 21681776]
35. Wang HH, Wang L, Jerde TJ, et al. Characterization of autoimmune inflammation induced prostate stem cell expansion. Prostate. 2015; 75:1620–1631. [PubMed: 26174474]
36. Boothroyd JC, Black M, Bonnefoy S, et al. Genetic and biochemical analysis of development in *Toxoplasma gondii*. Philos Trans R Soc Lond B Biol Sci. 1997; 1352:1347–1354.
37. Hahn AM, Myers JD, McFarland EK, Lee S, Jerde TJ. Interleukin-driven insulin-like growth factor promotes prostatic inflammatory hyperplasia. J Pharmacol Exp Ther. 2014; 351:605–661. [PubMed: 25292180]
38. Sherwood ER, Theyer G, Steiner G, Berg LA, Kozlowski JM, Lee C. Differential expression of specific cytokeratin polypeptides in the basal and luminal epithelia of the human prostate. Prostate. 1991; 18:303–314. [PubMed: 1711687]
39. Anja PM, Verhagen Frans CS, Ramaekers Tilly W. Colocalization of basal and luminal cell-type cytokeratins in human prostate cancer. Cancer Res. 1992; 52:6182–6187. [PubMed: 1384957]
40. Derouin F. Pathogeny and immunological control of toxoplasmosis. Braz J Med Biol Res. 1992; 25:1163–1169. [PubMed: 1341911]

41. Courret N, Darche S, Sonigo P, Milon G, Buzoni-Gatel D, Tardieux I. CD11c- and CD11b-expressing mouse leukocytes transport single *Toxoplasma gondii* tachyzoites to the brain. Blood. 2006; 107:309–316. [PubMed: 16051744]
42. Serhan CN, Chiang N, Van Dyke TE. Resolving inflammation: dual anti-inflammatory and pro-resolution lipid mediators. Nat Rev Immunol. 2008; 8:349–361. [PubMed: 18437155]
43. Ofner P, Bosland MC, Vena RL. Differential effects of diethylstilbestrol and estradiol-17β in combination with testosterone on rat prostate lobes. Toxicol Appl Pharmacol. 1992; 112:300–309. [PubMed: 1539166]
44. Tangbanluekal L, Robinette CL. Prolactin mediates estradiol-induced inflammation in the lateral prostate of Wistar rats. Endocrinology. 1993; 132:2407–2416. [PubMed: 8504745]
45. Kwon OJ, Zhang L, Ittmann MM, Xin L. Prostatic inflammation enhances basal-to-luminal differentiation and accelerates initiation of prostate cancer with a basal cell origin. Proc Natl Acad Sci USA. 2014; 111:E592–E600. [PubMed: 24367088]
46. Shinohara DB, Vaghasia AM, Yu SH, et al. A mouse model of chronic prostatic inflammation using a human prostate cancer-derived isolate of *Propionibacterium acnes*. Prostate. 2013; 73:1007–1015. [PubMed: 23389852]
47. Rudick CN, Berry RE, Johnson JR, et al. Uropathogenic *Escherichia coli* induces chronic pelvic pain. Infect Immun. 2011; 79:628–635. [PubMed: 21078846]
48. Simons BW, Durham NM, Bruno TC, et al. A human prostatic bacterial isolate alters the prostatic microenvironment and accelerates prostate cancer progression. J Pathol. 2015; 235:478–489. [PubMed: 25348195]
49. Haverkamp JM, Charbonneau B, Crist SA, et al. An inducible model of abacterial prostatitis induces antigen specific inflammatory and proliferative changes in the murine prostate. Prostate. 2011; 71:1139–1150. [PubMed: 21656824]
50. Sfanos KS, De Marzo AM. Prostate cancer and inflammation: the evidence. Histopath. 2012; 60:199–215.

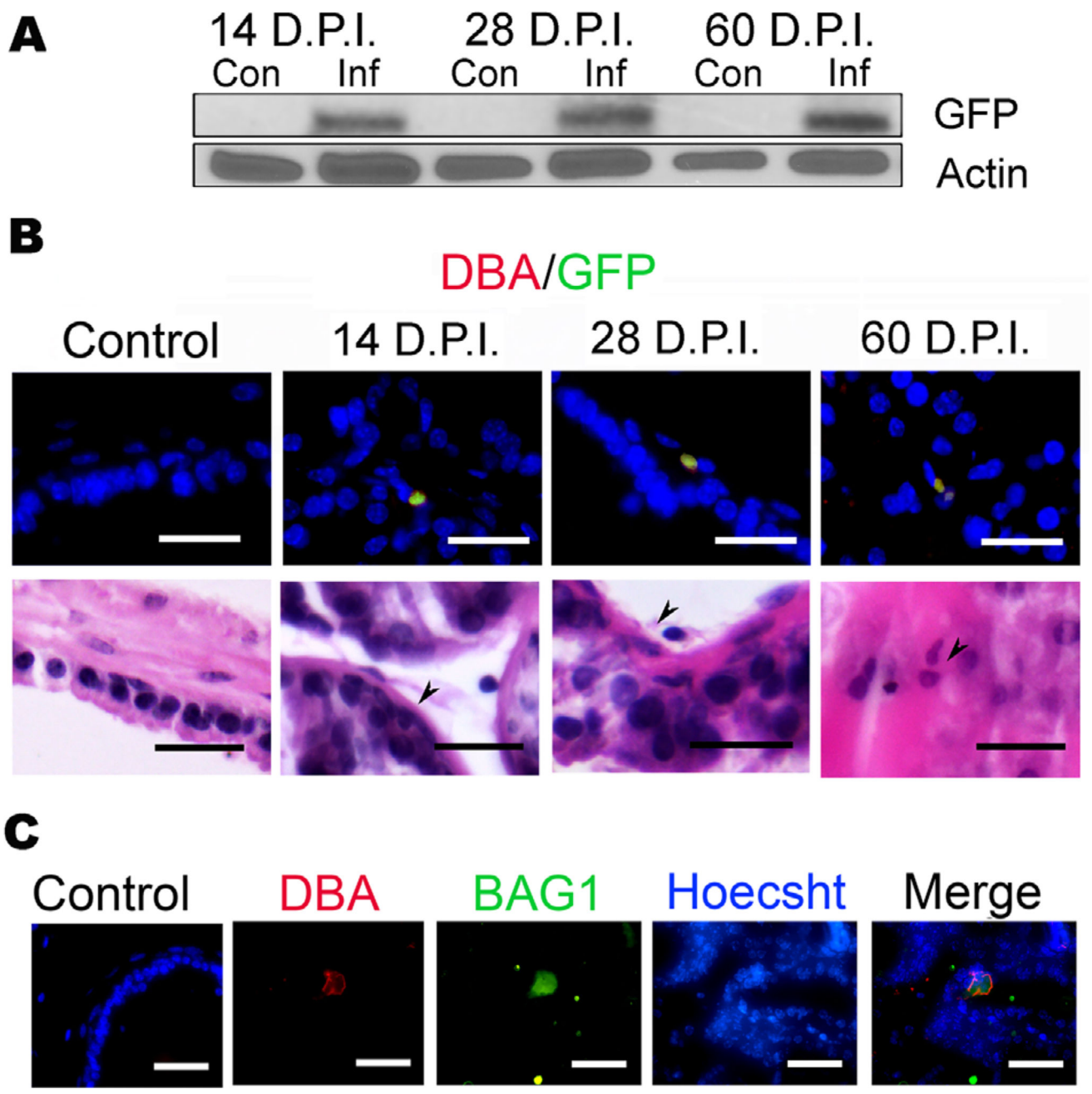

FIGURE 1.

T. gondii chronically encysts in the mouse prostate. Male CBA/J Mice were injected intraperitoneally with either sterile PBS or 40 000 PruΔhpt + ldhGFP *T. gondii* tachyzoites, and euthanized at either 14 (n = 14), 28 (n = 16), or 60 (n = 6) days post infection (DPI), and their brains and prostates were collected. (A) *T. gondii* localization and encystation in the mouse prostate was confirmed by detection of *T. gondii*-expressed GFP by Western blot analysis of protein extracts from either uninfected control mice (Con) or infected mice (Inf) at the time indicated. (B) *T. gondii* localization and chronic encystation in the mouse prostate was visualized by immunofluorescence in all infected mice prostates at 14, 28, and 60 DPI. Dorsal lateral prostate (DLP) sections from infected mice for the time indicated

were co-stained for *T. gondii*-expressed GFP (green) and the *T. gondii* specific cyst wall marker *Dolichols biflorus agglutinin* (DBA) conjugated to rhodamine (red).[36] Arrow heads denote *T. gondii* cysts; scale bars mark 25 μm. Serial section of the GFP/DBA stained slides, stained with hematoxylin and eosin (H&E). Arrow heads denote *T. gondii* cysts; scale bars mark 25 μm. (C) To confirm specificity of *T. gondii* labeling, 60 days prostates were co-stained with bradyzoite antigen (Bag1), the parasite specific heat shock protein, Hsp30 (green), and DBA (red) and are shown in an 80× image.[33] Scale bars represent 25 μm

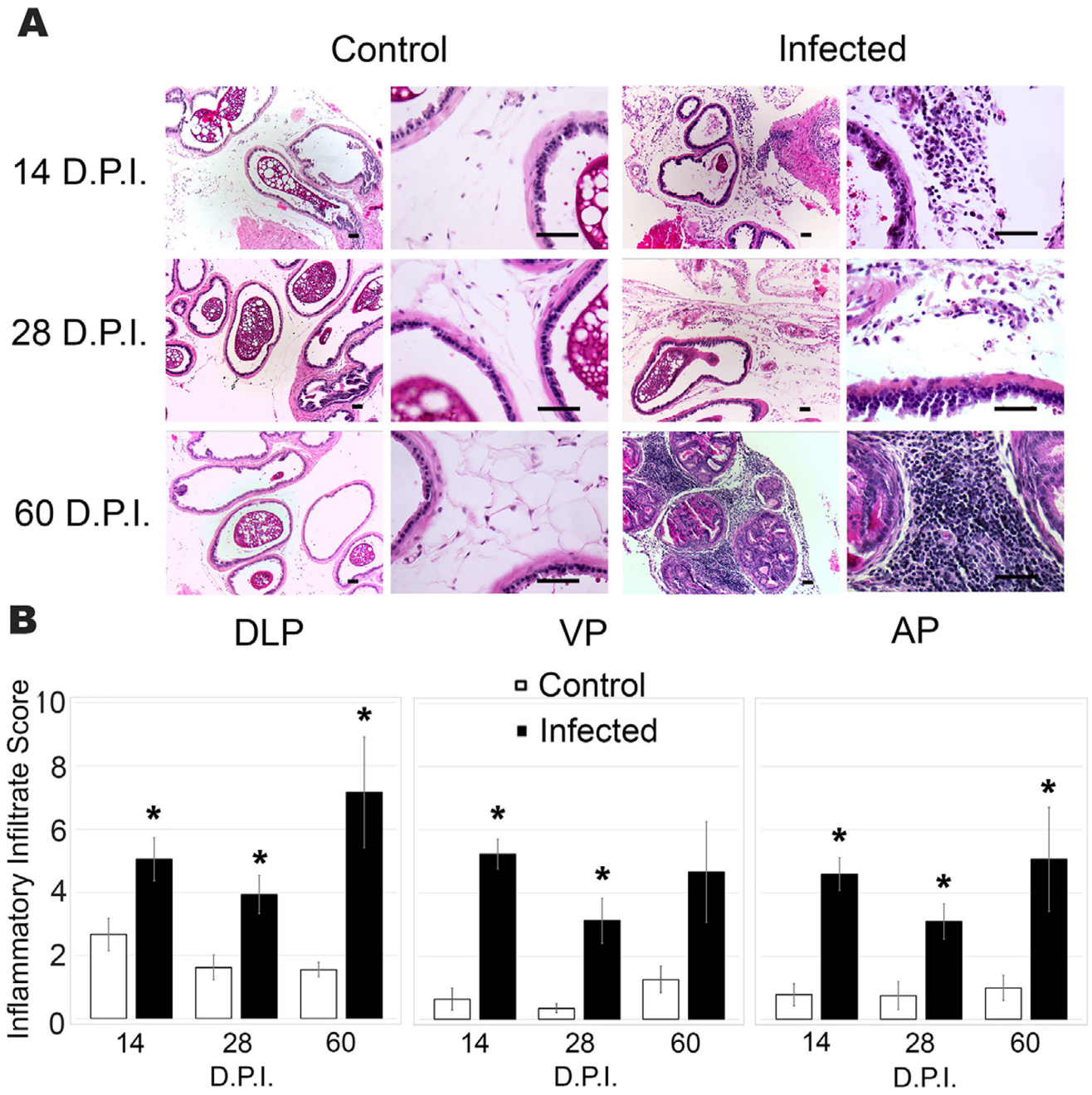

FIGURE 2.

T. gondii infection induces acute and chronic inflammatory responses in the mouse prostate. (A) Representative 10× (left) and 40× (right) images of (H&E)-stained sections of dorsal lateral prostates (DLP) from uninfected control (left) and *T. gondii* infected (right) mice at 14, 28, and 60 DPI Scale bars mark 25 μm. (B) Inflammatory infiltrate scores from DLP, ventral (VP), and anterior lobes (AP) of age-matched control and *T. gondii* infected mice at 14, 28, and 60 DPI, (n = 6–10, each group) using the established scoring system published by Boehm et al.[34] Data are presented as the mean inflammatory infiltrate score ± SEM and compared to uninfected control mice by two-tailed student's t-test. *$P < 0.05$

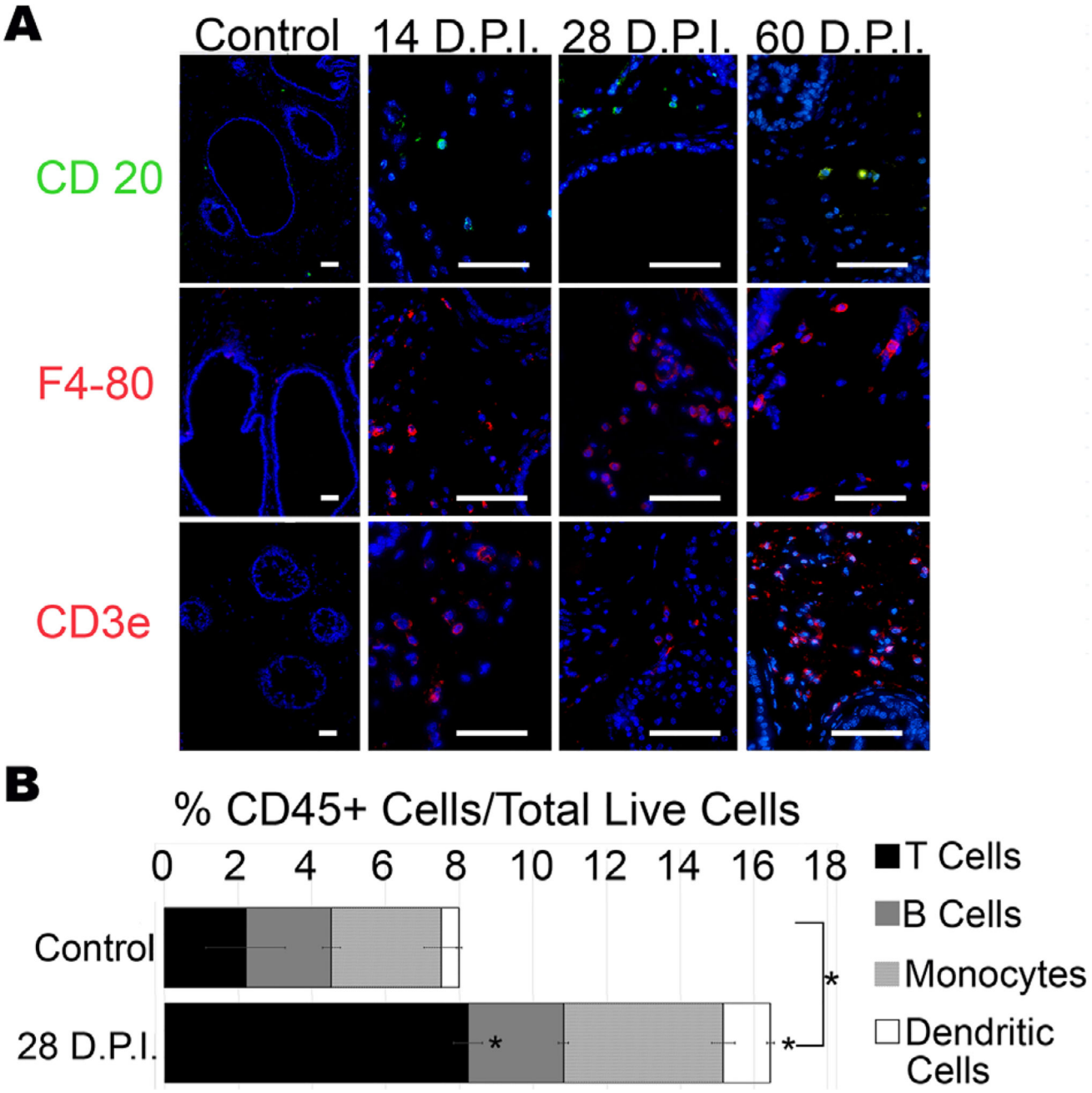

FIGURE 3.

Chronic *T. gondii* infection of the mouse prostate induces monocytic and lymphocytic infiltrate. (A) Representative immunofluorescent images of inflammatory infiltrate in the DLP of control (uninfected age-matched) and T. gondii-infected mice at 14 ($n = 6$), 28 ($n = 10$), and 60 ($n = 5$) DPI stained with the B-cell marker CD20 (top, green), the monocyte marker F4-80 (middle, red), and the T-cell marker CD3ε (bottom, red). Scale bars mark 25 μm. (B) Quantification of immune cells within the CD45+ population by flow cytometry. Data shown are the ratio of total inflammatory cells to total live cells (whole bar length), and the ratio to total live cells of CD3ε+ T lymphocytes (black portion of the bar), CD20+ B

lymphocytes (grey portion), F4-80+ monocytes (hatched portion), and Cd11c+/CD8α+ dendritic cells (white portion) in *T. gondii*-infected and age-matched control mice at 28 DPI. Data are presented as mean ratio to total live cells ± SEM; infected and control groups were compared by two-tailed student's *t*-test. $*P < 0.05$ ($n = 6$)

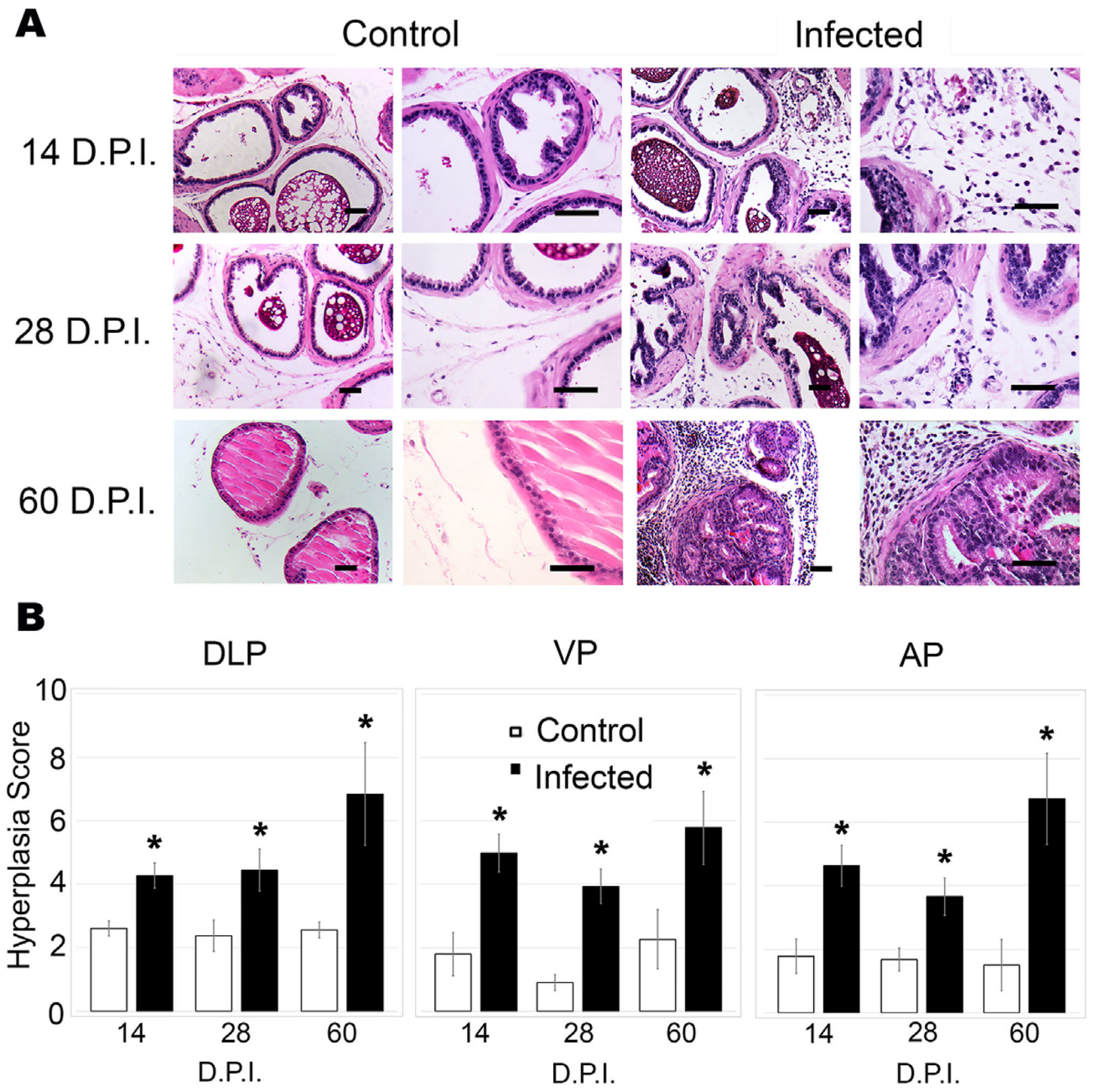

FIGURE 4.

Prostatic inflammation induced by *T. gondii* results in reactive hyperplasia. (A) Representative 20× (left) and 40× (right) images of H&E-stained DLPs from uninfected control (left) and *T. gondii*-infected (right) mice at 14, 28, and 60 DPI. Scale bars mark 25 μm. (B) Hyperplasia scores from DLP, VP, and AP of age-matched-control and *T. gondii*-infected mice at 14, 28, and 60 DPI (n = 6–10, each group) using the scoring system established by Boehm et al.[34] Data are presented as the mean hyperplasia score ± SEM. Infected mice are compared to uninfected control mice by two-tailed student's t-test. *P < 0.05

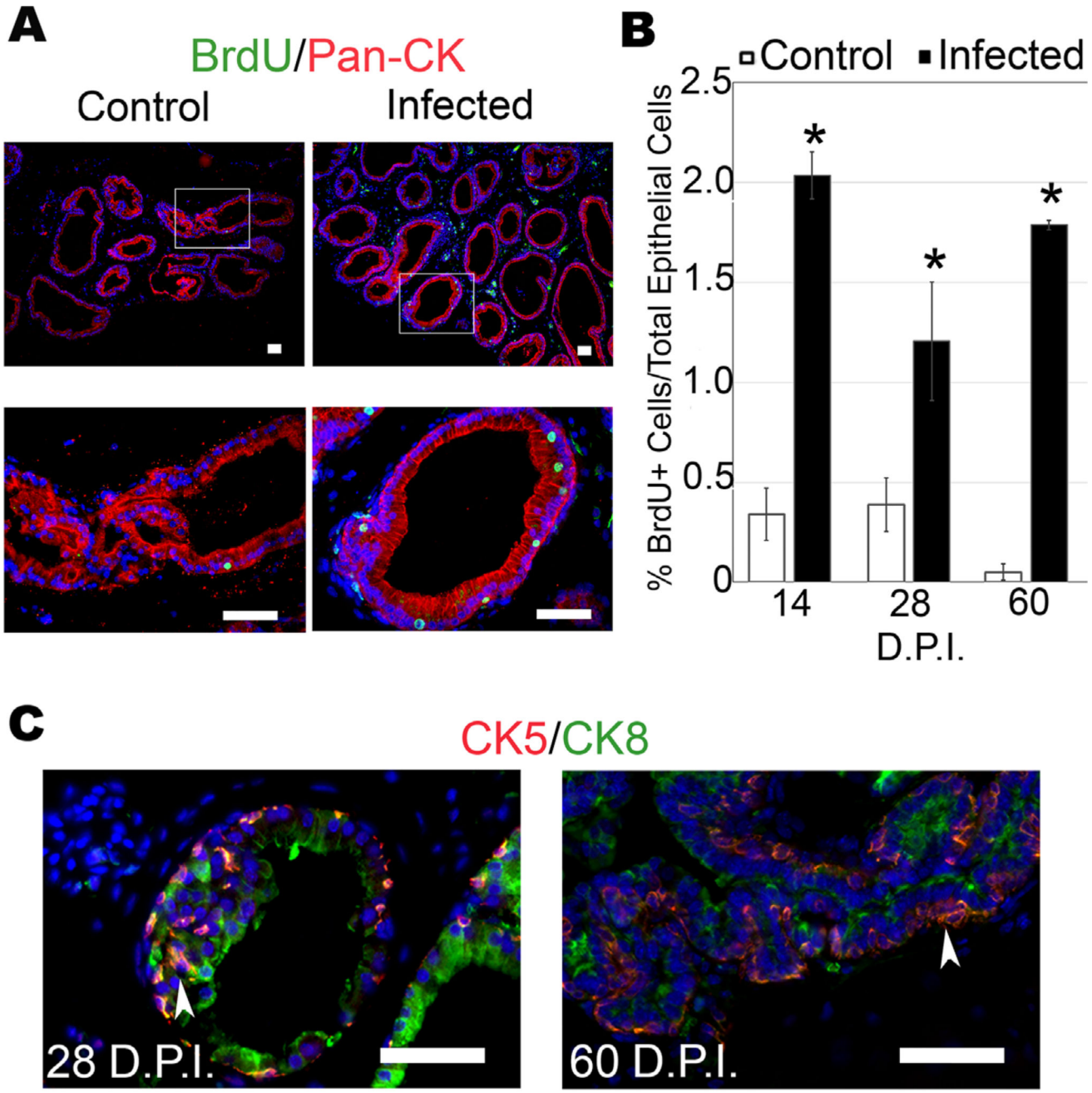

FIGURE 5.

T. gondii-induced reactive hyperplasia exhibits epithelial proliferation, expansion of transit amplifying cells, and proliferative microglandular hyperplasia in chronically infected prostates. Proliferation in *T. gondii*-infected and control mice was determined by BrdU-labeling 2 h prior to sacrifice followed by immunofluorescence. (A) Representative BrdU staining at 28 DPI. BrdU (green), pan-cytokeratin (red), scale bars indicate 25 μm. (B) Quantified data of BrdU-positive epithelial cells from infected and control prostates harvested at 14 ($n = 6$), 28 ($n = 6$), and 60 ($n = 4$) DPI. Three random 20× views/mouse prostate were quantified and averaged as percent proliferating (BrdU+) epithelial cells to

total epithelial cells in the field of view. Data are presented as the mean % BrdU+ epithelial cells ± SEM in each group. Infected mice are compared to age-matched control by two-tailed student *t*-test; $*P < 0.05$. (C) Expansion of epithelial transit amplifying cells (TACs) determined by cytokeratin 5 and 8 co-immunofluorescent staining. Representative *T. gondii*-infected 28 and 60 days mouse prostates immunostained with the basal epithelial marker cytokeratin 5 (CK5) (red) and luminal epithelial marker cytokeratin 8 (CK8) (green), as indicated by arrow heads. Scale bars represent 25 μm

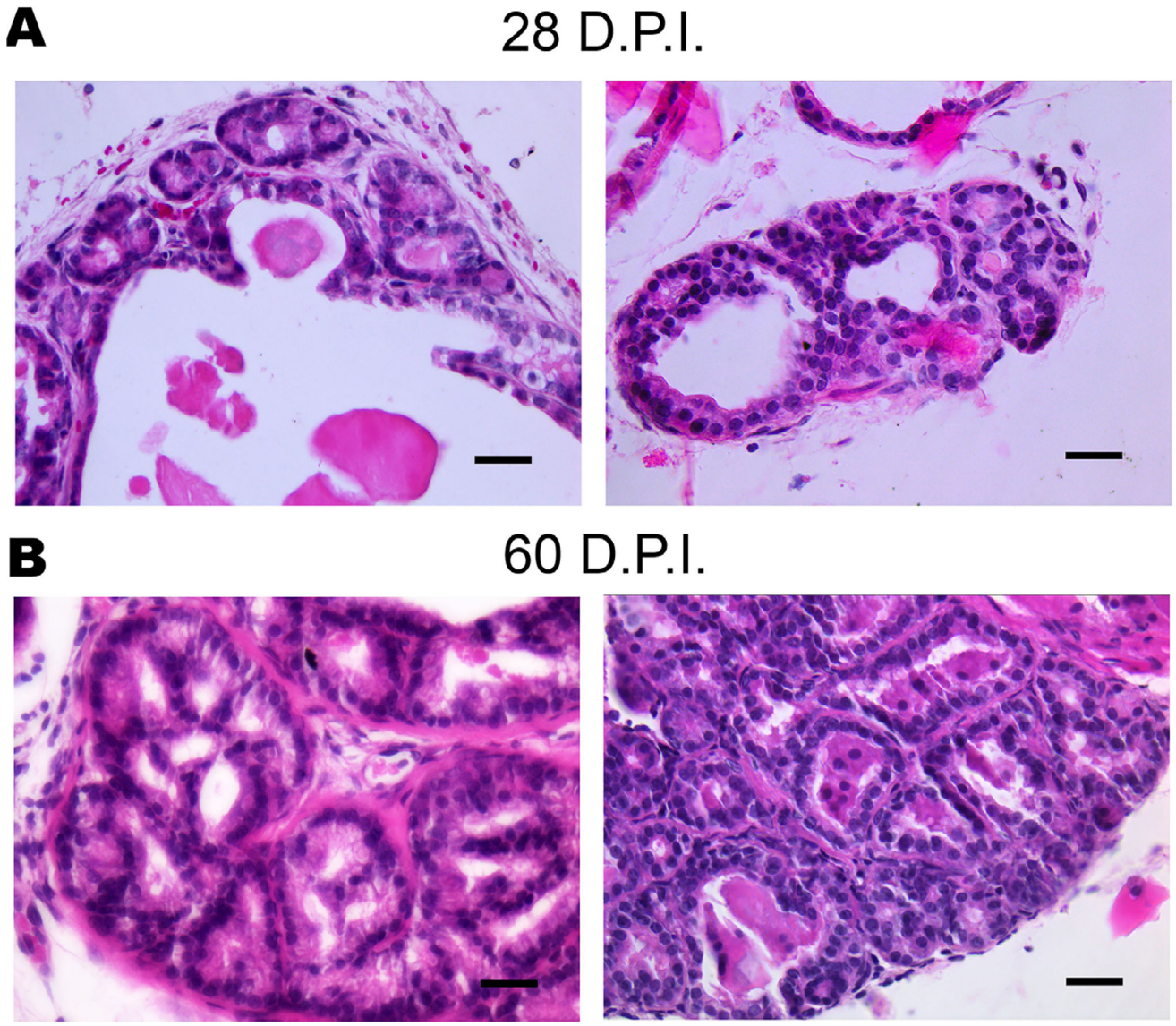

FIGURE 6.

Chronic *T. gondii* infection elicits proliferative inflammatory reactive microglandular hyperplasia in the mouse prostate at 28 (top) and 60 DPI (bottom). This phenotype is observed in 13/16 prostates at 28 DPI and is fully penetrant at 60 DPI ($n = 6$)